

An array of simple, fast, and safe approaches to visualizing fine cellular structures in free-hand sections of stem, leaf, and fruit using optical microscopy

Bhaskar R. Bondada

Washington State University Tri-Cities, Department of Horticulture and Landscape Architecture, 2710 Crimson Ave, Richland, WA 99354, USA.

Abstract

A wide array of free-hand-sectioning-based optical microscopy techniques that are simple, safe, and inexpensive, yet allows quick and easy identification of specific cell types and cellular components with unprecedented resolution are presented using leaf (*Saintpaulia ionantha* and *Schefflera actinophylla*), stem (*Vitis vinifera* and *V. labruscana*), and fruit (*Vitis vinifera*) tissues. The objective of this study was to generate contrast and capture high quality cellular images of various plant organs either via infusing basic fuchsin, a xylemic dye into organs or using naturally pigmented organs by employing the classic technique of free-hand sectioning. Also, images were obtained via post-staining free-hand sections of organs without any dye infusion. Leaves injected with dye revealed its strikingly regular and hierarchical reticulate venation structure. The free-hand sections of healthy and water-stressed leaf petioles, and stems and pedicels prepared from organs either infused with basic fuchsin or post-stained with safranin displayed exceptional cellular details. These included the xyletic and phloic transport systems positioned around the central parenchymatous pith, their tissue pattern in each system, and occlusion of xylem vessels by the parenchymatous tissues (tylosis). The free-hand sections of fruit revealed fine details of its translucent mesocarp embedded with vasculature of varied architecture, and seed morphology. Free-hand sections of naturally chromated petioles illustrated its internal structure pertaining to anthocyanin accumulating cells and crystals in superb details, and particularly, the most visually spectacular images of trichomes. Since observations of internal structures of plants constitute the foundations of plant biology, the microscopy techniques illustrated in this study can be of great interest and benefit to both addressing fundamental questions in plant biology and curiosity-driven research.

Keywords: Optical microscopy, Free hand section, stem, fruit, leaf

INTRODUCTION

Ever since Anton van Leeuwenhoek made significant advances in microscope design and use, microscopes have become a requisite magnifying and analytical tool in most scientific investigations. Of the wide array of microscopes available today, optical microscopy is the norm in all realms of science because of its sheer simplicity. Typically, optical microscopy involves examining the specimens that have been killed by fixation and then dehydrated, embedded in a solid matrix, sectioned, stained, and finally observed with an optical microscope [10, 14, 46]. However, such lengthy processing promotes autolysis and putrefaction causing tissue deformation and other artifacts [63]. Conversely, free-hand sectioning, a process of making sections of fresh samples by hand using a razor blade [46] eliminates such deformation problems, yet allows fresh and often unexpected insights into cellular organization. Such competence appeals to plant biologists who frequently employ this technique as an alternate method of microtomy for describing, defining and refining cell-biological questions. Overall, it provides an adequate method for rapid and inexpensive microscopic

observation of their internal structure [39].

As plant tissues have little inherent contrast and lack color, the success and imaging of cell structures by free-hand sectioning are largely reliant on reactive organic dyes. These dyes are basically coloured substances dissolved in liquids that impart their colouring effect by staining or being absorbed by cell components. Following staining, contrast occurs, i.e. the stained tissue appears colored and superimposed over a light background, which essentially enhances visualization of specific intra- or extracellular elements within tissues allowing the human observer much useful information about tissue composition [44]. Often the dyes used in staining have an affinity for a specific tissue element, consequently the selection of dyes depends upon the nature of the desired cell components. For instance, the protein stain Toluidine Blue O and the fluorochrome Acridine Orange are particularly good general stains for tissue sections from fresh and embedded tissue [37]. Another commonly used dye in plant histology and general cytology is safranin, a cationic dye, which has long been used in combination with fast green as a counter stain [46].

An increasing repertoire of free-hand sectioning techniques (e.g. clearing and staining free-hand sections) have evolved since the dawn of microscopy. While yielding good microscopic images, most of them often rely on use of toxic clearing solutions [15, 39] such as chloral hydrate [52] and complex staining process rendering this simple technique unsafe, labor intensive and time consuming [3]. Most importantly, the existing literature on free-hand sectioning is limited to roots [18, 39], not much free-hand sectioning has been practiced with other plant organs such as woody stem, leaf and especially fleshy fruits. In view of these

Received: Dec 17, 2011; Revised: Jan 05, 2012; Accepted: Jan 21, 2012.

*Corresponding Author

Bhaskar R. Bondada

Washington State University Tri-Cities, Department of Horticulture and Landscape Architecture, 2710 Crimson Ave, Richland, WA 99354, USA.

Tel: +509-372-7348; Fax: +509-372-7391

Email: bbondada@wsu.edu

shortcomings, alternative or complementing approaches such as staining of cellular components in live organs by injecting dye through cut ends are required to permit their identification in organs other than roots. Alternatively, free-hand sections can be prepared from organs that naturally accumulate colored secondary metabolite pigments such as anthocyanins [50] or organs that change color with season [4] or post-stain the sections with fluorochrome such as 5 (6)-carboxyfluorescein diacetate (CFDA) [11]. The dyes that can stain live organs include anionic and cationic forms of fuchsin [13, 35, 48], which are generally used to elucidate the water conducting pathways in living trees [48, 61]. However, the contrast ensuing from dye uptake can be exploited in free-hand sections for obtaining a rapid static snapshot of cellular structures. The objective of this study was to revisit the classic technique of free-hand sectioning and show cellular structures in brilliant details in fresh sections of woody stems, leaves, and fleshy fruit tissues that have been either infused with dye or they had natural accumulation of color compounds in their cells.

MATERIALS AND METHODS

Plant material

Different plant species were used for this study: these included *Schefflera actinophylla*, African violet (*Saintpaulia ionantha*), and field-grown (*Vitis labruscana*) and greenhouse grown (*Vitis vinifera*) grapevines. The rationale for selecting this ensemble of plants is that they represent popular species' commonly used as model plants to gain an understanding of propagation principles and techniques (African violet and *Schefflera* plant) and to elucidate the physiology of woody perennials (grapevines). Young African violet plants were obtained from local nursery and were maintained in the laboratory at 28 °C by fertilizing weekly with 150 ppm of 20:20:20 Peters® fertilizer (Peters Fertilizer Products, W. R. Grace & Co., Allentown, PA) in deionized water. The plants received 9 h of light each day from a 40-w Grow-Lux (Sylvania) fluorescent lamp. The leaves of the African violet had a dark green adaxial surface and purple abaxial surface, respectively. The *Schefflera* plant was also obtained from local nursery and maintained in the laboratory under similar growth conditions as the African violet. One set of plants were watered regularly to maintain healthy leaves while another set was water stressed by withholding water. Once the lower leaves displayed water stress symptoms (wilting), watering was resumed to maintain the plants in a healthy condition. Shoots of healthy grapevine (*Vitis labruscana*) were sampled from local vineyard, whereas shoots afflicted with physiological disorder entailing green stem with no leaves were sampled from greenhouse grown grapevines (*Vitis vinifera*). They were cut using a pruner and immediately brought to laboratory with its cut end immersed in a flask filled with water for infusing the dye.

Dye infusion into leaves, stem and berries

For passive dye infusion, the technique employed by Bondada et al. (2005) [13] was used. Briefly, well-watered (Figure 1A) and water-stressed leaves (Figure 1B) of the *Schefflera* plant were excised and the cut end of the petiole was immediately dipped in a small reservoir of an apoplastic dye (basic fuchsin 0.1% aqueous) [59]. The reason for selecting basic fuchsin over acid fuchsin was that basic fuchsin unlike its counterpart adheres to cell wall and does not wash out during tissue preparation [48]. Infusion through the cut petiole was allowed to occur for about one hour

under laboratory conditions. Similarly, woody grapevine shoots and young grape berries were infused with the same dye.

Post-staining with safranin

Free-hand sections of green stems of grapevine were post-stained with safranin O (Fisher Scientific, Pittsburgh, PA), 0.5% (w/v) dissolved in 50% EtOH and viewed with bright field microscopy. Similarly, free-hand sections of grape pedicels were post-stained with safranin O, but these were observed with wide field epifluorescence microscopy.

Staining with 5 (6)-carboxyfluorescein diacetate (CFDA)

Free-hand sections of African violet leaf petioles were stained with 10 µM solution of CFDA (Invitrogen Corporation, Carlsbad, CA) (prepared from a stock solution of CFDA in dry dimethyl sulfoxide, DMSO containing 5 mg of CFDA/ml of DMSO) for 15 minutes and observed with epifluorescence microscopy.

Cellular staining due to natural chromation by anthocyanins

Free-hand sections of purple African violet leaf petioles were observed with bright field microscopy to obtain high contrast images of cellular details of petioles, and with epifluorescence microscopy to capture fluorescing images of trichomes. In a similar manner, the pigmented (red) grapevine leaves (red color due to seasonal changes) and ripened grape berries that accumulate anthocyanins in their septum and brush region were treated to view cellular details of petioles and internal vascular architecture of berries using bright field microscopy.

Free-hand sectioning

Samples for observation with bright field and epifluorescence microscopy were prepared by using standard free-hand sectioning technique as described by Ruzin (1999) [46]. All sections were cut using a new double-sided razor blade. In the case of stem and leaf petioles, first, a leveling cut was made for the purpose of forming a right angle with the axis of the organ to ensure that the sections made were cross sections. After each cutting, the cut section that collected on the blade were transferred to a drop of water on a slide and covered with a cover slip by lowering it an angle onto the drop of water containing the sections. Berries were cross-sectioned at the proximal and distal ends and sectioned longitudinally through the center for observation with stereomicroscopy.

Microscopy

Observation of sections involved stereomicroscopy (Stemi 2000-C, Carl Zeiss Inc., Thornwood, NY, USA), bright field microscopy (Axioskop 2 Plus, Carl Zeiss Inc., Thornwood, NY, USA), and wide-field epifluorescence microscopy (Axioskop 2 Plus, Carl Zeiss Inc.) with fluorescence excitation at 365 nm using the emission filter long pass 420 nm (Carl Zeiss Inc.). Images were recorded using a DXM 1200C digital camera (Nikon Instruments Inc., Melville, NY, USA).

RESULTS

As expected, the *Schefflera* leaf petiole without any dye infusion exhibited colorless cortical and vascular tissues (Figures 1(a), 1(b)). Following the infusion of basic fuchsin into leaves, the water-stressed *Schefflera* leaf showed limited dye distribution, which primarily confined to green lamina (Figure 1(c)). Conversely, the dye was distributed throughout the healthy leaf revealing its strikingly regular and hierarchical structure, commonly known as reticulate venation (Figures 1(d), 1(e)). In this type of vascular architecture, the mid vein ramified palmately confining anastomoses (veins which are primarily cylindrical bundles of vascular tissues of many sizes) and areola, which terminated the veins and together they constructed a reticulate venation pattern in the intercostal (between veins) regions (Figure 1(d)). Staining of major and minor veins including the terminal vein endings serving the polygons of areolae was clearly visible throughout the healthy leaves (Figure 1(e)). Furthermore, this particular leaf displayed open ending veinlets consisting of multiple (generally two) tracheary elements (probably tracheids). Transverse section through the petiole revealed collateral vascular bundles consisting of centripetally directed xylem and centrifugally directed phloem capped by a ridge of sclerenchymatous fibers were arranged as a ring of separate vascular bundles around a pseudo-pith resembling the pith in dicotyledonous stems (Figure 1(f)). The vessels and the xylary fibers were clearly distinguishable due to staining of their walls (Figure 1(f)). With a green filter in the light path, only the lumen of the vessels and fibers could be clearly distinguished as the filter imparted a bright greenish luminescence to the lumens (Figure 1(g)). On the contrary, the xylary fiber cell walls and the lignified secondary cell walls of sclerenchymatous phloem fiber cap positioned in the periphery of the primary sieve elements appeared dark (Figure 2(a)), whereas the middle lamella of the phloem fibers had a faint greenish luminosity to it (Figure 2(b)). Apparently, the vascular tissues had a better resolution in the presence of a green filter in the light path. The secondary cell walls were evenly deposited on the inside of the primary walls (Figure 2(b)). Such deposition of walls reinforces these cells allowing them to function as mechanical tissues for structural support and protection, as well as enabling tracheary elements to withstand the negative pressure generated during transpiration. The walls of parenchymatous pith were also stained (Figures 3(a), 3(c)), which appeared dark under a green filter (Figure 3(b)). On the contrary, when illuminated with UV light, the stained walls elicited a yellowish fluorescence significantly enhancing the image quality (Figure 3(d)). In contrast to healthy *Schefflera* leaves, the dye did not ascend towards the distal end of water-stressed *Schefflera* leaf, rather it was confined to the proximal end at the petiole and midrib (Figure 1(c)). Nevertheless, limited staining of xylem tissues was detected in the unstained midrib region that appeared colorless visually although few outer vessels and phloem fibers were stained (Figure 3(e)). The stained region of the petiole and midrib was similar to healthy leaves.

Although the pith, xylem vessels, ray parenchyma, and phloem tissues were visible in the unstained sections of grapevine stem when observed with bright field microscopy, overall it had a poor contrast in the absence of dye uptake through the xylem (Figure 4(a)). On the other hand, the elegant pattern of the vascular tissues were clearly distinguishable in the sections obtained from stems injected with dye, which resulted in high contrast and clear images displaying the secondary conducting tissues (Figures 4(b),

4(c)). For instance, it can be clearly seen that this particular stem had initiated secondary growth, a developmental process driving radial expansion by forming secondary phloem centrifugally and secondary xylem (woody structures) centripetally. The cluster of centripetal secondary xylem vessels embedded in the xylary fibers and separated by radiated bands of parenchyma cells were open and thus their lumens were clearly visible (Figures 4(b), 4(c)). The centrifugal secondary phloem displayed alternating bands of soft phloem (parenchymatous tissues) and hard phloem (fibers) (Figure 4(d)). On the other hand, primary phloem comprised of parenchymatous tissues bounded by fiber cap (Figure 4(e)) was crushed by the phellem (Figure 4(f)). These extraxylary fibers consisted of cluster of fibers whose cross section resembled that of a porous kidney-shaped framework wherein the thickened secondary cell walls filling the lumen appeared light yellowish in color and were separated by shiny yellowish middle lamella (Figure 4(e)). Just like in the petiole fiber cap, the secondary cell walls were evenly deposited on the inside of the primary walls.

The safranin-stained free-hand transverse sections of young green grapevine stem replete with tylosed xylem vessels observed under white light displayed red stained cell walls in fibers and parenchyma cells that occluded the xylem vessels (Figures 5(a), 5(b)). Conversely, when safranin-stained grape pedicel sections were illuminated with UV light, the discontinuous ring of phloem fiber cap consisting of a single layer of cells (Figure 6(a)), the xylary fibers, and xylem vessels (Figures 6(b), 6(c), 6(d)) radiated luminous yellow fluorescence, whereas the ray parenchyma cells showed faint yellow fluorescence (Figure 6(b)).

Longitudinal and transverse sections of young grape berries infused with dye displayed nice details of its vascular architecture, which basically originated from the pedicel as a group consisting of three components and ramified in the dorsal and ventral regions of the mesocarp (Figures 6(e), 6(f)). One of the components, the axial vascular bundle extended into the distal pole of the berry (Figure 6(e)). The second component, the highly ramified peripheral or dorsal vascular bundle branching out from the axial vascular bundle at the proximal end (Figure 6(e)) and then again uniting with the axial vascular bundle at its distal end (Figure 6(e)) was located just beneath the exocarp. The third component entailed the ovular vascular bundles that served the seeds (ovules) (Figure 6(e)). The peripheral vascular bundle, i.e. the branchings of axial vascular bundle subdivided the outer mesocarp into a series of polygons of different sizes, which in longitudinal face view resembled a reticulum (Figure 6(f)). Since the peripheral vascular bundles originated from the proximal end of axial vascular bundle and then united at the distal end of the axial vascular bundle, their centrifugal radiation and centripetal union could be seen in transverse sections taken at the proximal and distal poles of the berries (Figures 7(a), 7(b)). Unlike the young berries, the dye could not be infused into the ripened berries, nevertheless their vasculature design similar to the young berries was clearly visible (Figures 7(c), 7(d)). The anthocyanins that accumulated in the brush and septum regions resulted in high contrast and made possible clear images of their vascular network in the translucent mesocarp. In fully ripened berries, the seeds were brown in color resulting from tannin accumulation in the seed integuments (Figure 7(c)). Since they are embedded in the translucent mesocarp, it was possible to observe some of its morphological features such as its shape and raphe (Figure 7(d)).

The transverse sections of African violet leaf without any dye infusion when observed with bright field microscopy revealed

colorless covering and glandular trichomes against a outer chromated surface and a colorless inner surface (Figures (8a), (8b)). The trichomes occurred on a multicellular emergence (Figure (8b)). The chromation of the surface ensuing from the epidermal and hypodermal cells imparted both contrast to the tissues as well as highlighted the surface cells (Figure (8c)). Analogous to African violet, the grapevine leaf petiole displayed nice details of its internal structure due to the presence of chromated cells in the outer and inner regions of its structure (Figures (8d), (8e), (8f)). The chromation of cells mostly occurred in the hypodermal and inner cortical cells (Figures (9a), (9b), (9c)). While making transverse free-hand sections, some of the idioblasts were cut loose releasing druse and raphide crystals (Figure (9d)). The individual facets of the druse crystal displayed several distinct shapes such as oval, rectangle, diamond, and square as opposed to sole needle shaped raphide crystals (Figure (9d)).

Under white light, the trichomes of African violet were colorless (Figure (10a)); however, fluorescent images from UV illumination yielded spectacular view of the covering trichomes. The wart like structures on the surface of trichomes emanated a red auto fluorescence whereas a faint reddish fluorescence originated from their walls (Figures (10b), (10c)). A much better resolution of trichomes occurred with CFDA-induced fluorescence. It revealed fine details of cortical cells and a spectacular view of covering trichomes (Figures (10d), (10e)). The green fluorescence originating from carboxyfluorescein was visible in the thin peripheral layer of cytoplasm adjacent to the cell wall (Figure (10d)). The remarkable feature of the trichomes was yellow fluorescence emanating from a dense mass of warts at the region of septa and individual warts at the parietal walls (Figure (10d)). These trichomes were uniseriate and septated; most importantly were acicular (having the shape of a needle) (Figure 10)).

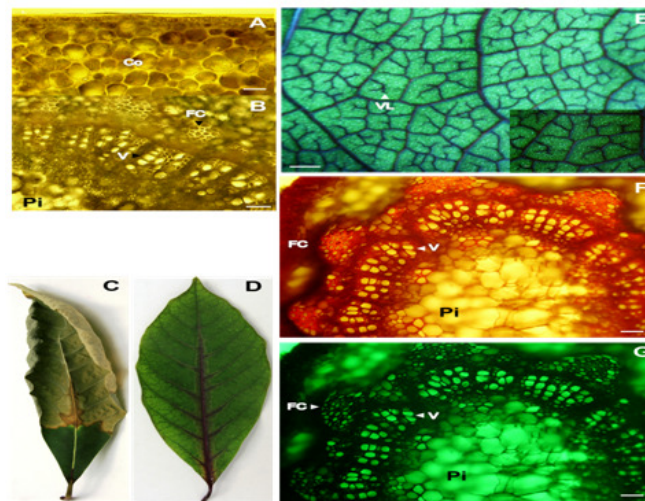


Fig 1. A free-hand transverse section of healthy *Schefflera* leaf petiole without any dye infusion exhibiting (A) colorless cortical and (B) vascular tissues, a photograph of (C) water-stressed *Schefflera* leaf infused with basic fuchsin dye showing limited dye distribution, which confined to green lamina, (D) a photograph of healthy *Schefflera* leaf infused with basic fuchsin dye showing dye distribution throughout the lamina, (E) micrograph of reticulate venation pattern in healthy leaf infused with dye (inset – high magnification of reticulate venation), (F) a free-hand transverse section of the healthy leaf petiole infused with dye and viewed with bright field microscopy showing the vascular tissues consisting of a ring of separate vascular bundles of unequal size embedded in the parenchyma tissue resembling a stem-type organization, (G) the same micrograph as in F viewed with bright field microscopy with a green filter in the light path. Scale bars: 25 μm (A), 50 μm (B), 500 μm (E), 50 μm (F-G). Co – Cortical cells, FC – Phloem fiber cap, Pi – Pith, V- Xylem vessels, and VL- Veinlet.

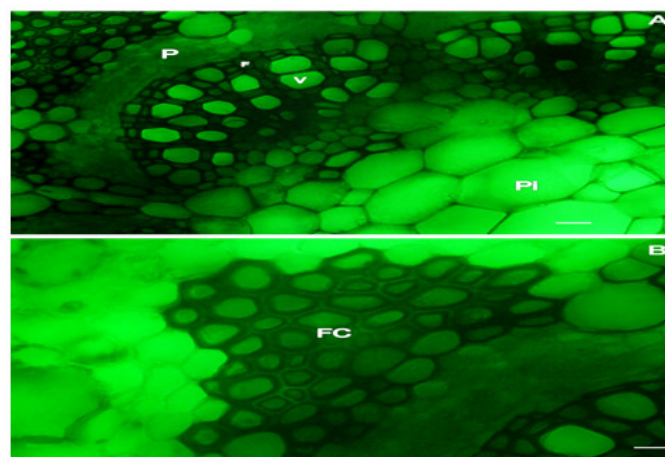


Fig 2. A free-hand transverse section of a single vascular bundle from a healthy *Schefflera* leaf viewed with bright field microscopy with a green filter in the light path showing primary phloem, fibers, xylem vessels and pith, (B) A free-hand transverse section of a phloem fiber cap viewed with bright field microscopy with a green filter in the light path showing the cell walls. Scale bars: 20 μm (A-B). F- xylary fiber, FC – Fiber cap, Pi – Pith, and V- Xylem vessels.

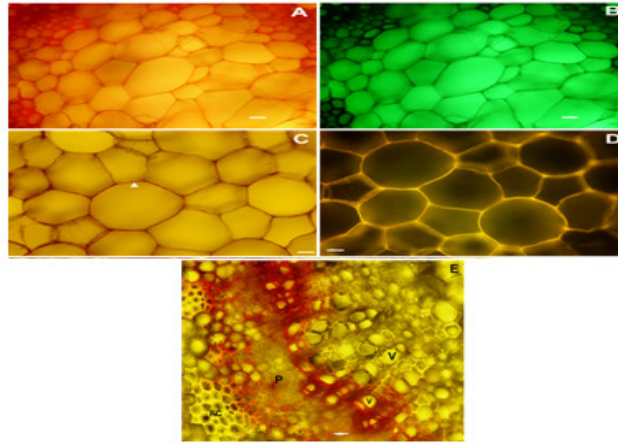


Fig 3. A free-hand transverse section of a healthy *Schefflera* leaf petiole showing pith viewed with (A) bright field microscopy and (B) bright field microscopy with a green filter in the light path, (C) high magnification of pith region viewed with bright field microscopy showing stained (safranin) cell walls (arrow head), (D) lower right hand portion of the micrograph (C) viewed with epifluorescence microscopy showing bright luminescent cell walls, and (E) A free-hand transverse section of a water-stressed leaf midrib from healthy region viewed with bright field microscopy showing staining (basic fuchsin) of cell walls in lower part of the fiber cap cells and upper part of the xylem vessels and fibers. Scale bars: 20 μ m (A-E). FC- Fiber cap, P- Phloem, and V- Vessels.

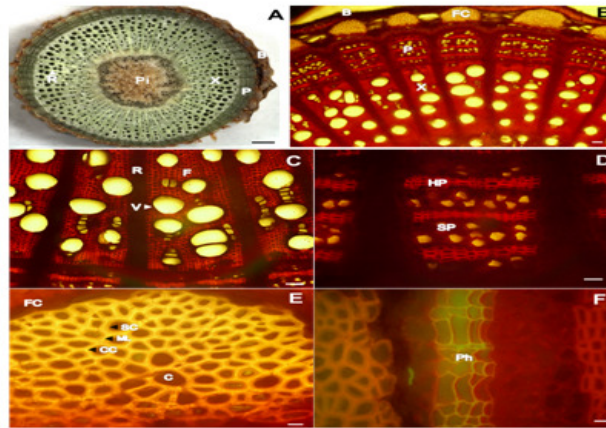


Fig 4. A free-hand transverse section of a woody grapevine stem (cane) without any dye infusion showing bark, secondary phloem, secondary xylem, ray parenchyma, and pith, (B) a high contrast micrograph prepared from a free-hand transverse section of a woody grapevine stem (cane) after infusing it with basic fuchsin showing bark, fiber cap, secondary phloem, and secondary xylem, (C) high magnification of (B) showing fibers, ray parenchyma, and xylem vessels, (D) secondary phloem showing alternate bands of hard phloem and soft phloem, (E) extraxylary fibers, the phloem fiber cap showing thick secondary cell wall, middle lamella and cavity where the protoplast was when these cells were alive), and (F) formation of phellogen in the phloem region. Scale bars: 500 μ m (A), 50 μ m (B-C), 25 μ m (D), 10 μ m (E-F). B- Bark, C- Cavity, CC- Cell corner, F- Finer, FC- Fiber cap, HP- Hard phloem, ML- Middle lamella, P- secondary phloem, Ph- Phellogen, Pi - Pith, R- Ray parenchyma, SC- Secondary cell wall, SF- Soft phloem, V- vessel, X- Secondary xylem.

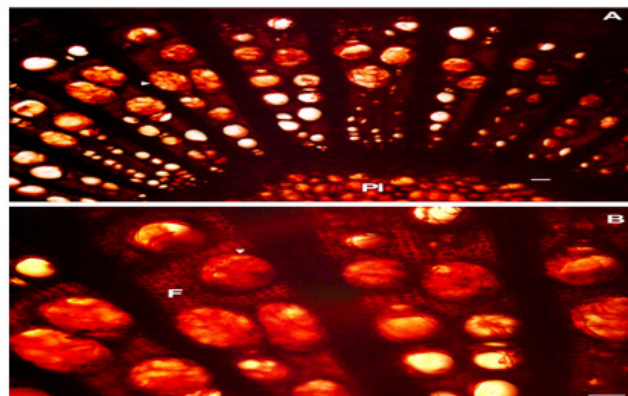


Fig 5. A free-hand transverse section of grapevine stem viewed with bright field microscopy showing (A) safranin post-stained tylosed xylem vessels (arrow head) and (B) high magnification of xylem vessels showing fibers and completely occluded xylem vessels (arrow head) with parenchyma cells. Scale bars: 50 μ m (A-B). F- Fiber cells, Pi- Pith.

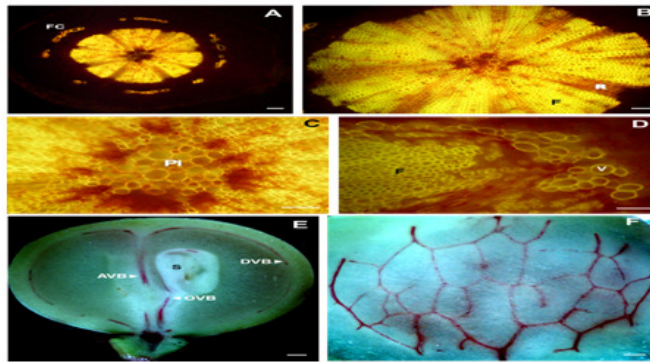


Fig 6. A free-hand transverse section of (A) grape pedicel post-stained with safranin and viewed with epifluorescence microscopy showing fiber cap and pith cells, (B) high magnification of (A) showing fibers and ray parenchyma cells, (C) high magnification of (B) showing pith parenchyma cells, a free-hand transverse section of (D) pedicel showing xylem vessels, a free-hand longitudinal section of (E) young grape berry infused with basic fuchsin and viewed with bright field microscopy showing internal architecture of vascular bundles (peripheral, axial, and ovular) and seed in the pericarp, and a free-hand longitudinal section of (F) young grape berry infused with basic fuchsin and viewed with bright field microscopy showing the peripheral vascular bundles. Scale bars: 50 μm (A-F). AVB- axial vascular bundle, DVB- dorsal vascular bundle, FC- Fiber cap, OVB- Ovular vascular bundle, Pi- Pith, R- Ray parenchyma, S- Seed, V- Xylem vessels.

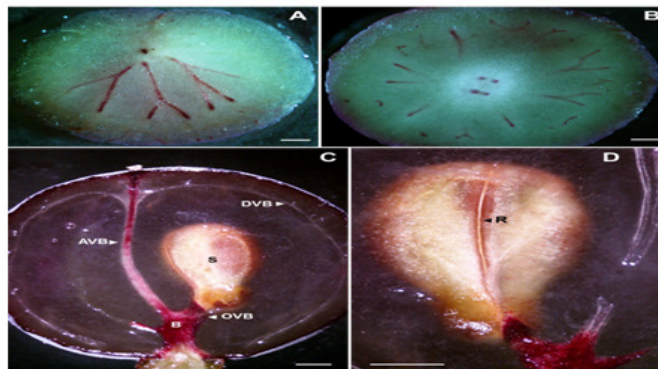


Fig 7. A free-hand transverse section of (A) young grape berry infused with basic fuchsin and viewed with bright field microscopy showing the architecture of vascular bundles at the distal (stylar) end of the berry, a free-hand transverse section of (B) young grape berry infused with basic fuchsin and viewed with bright field microscopy showing the architecture of vascular bundles at the proximal (pedicel) end of the berry, a free-hand longitudinal section of (C) ripened grape berry without any dye infusion viewed with bright field microscopy showing the internal architecture of vascular bundles and the position of seed in the translucent mesocarp and anthocyanin accumulation in the septum and brush regions, and a free-hand transverse section of (D) ripened grape berry without any dye infusion viewed with bright field microscopy showing a mature seed with raphe in the mesocarp. Scale bars: 500 μm (A, B) and 1 mm (C-D). AVB- axial vascular bundle, B- Brush, DVB- dorsal vascular bundle, FC- Fiber cap, OVB- Ovular vascular bundle, R- Raphe, and S- Seed.

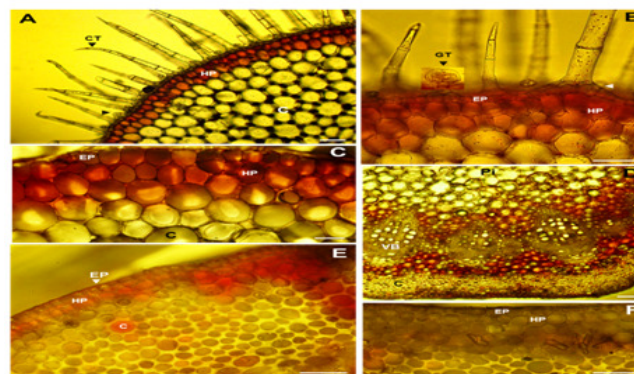


Fig 8. Free-hand transverse sections of (A) African violet leaf petiole without any dye infusion viewed with bright field microscopy showing colorless covering trichomes interspersed by glandular trichomes (arrow head), anthocyanin accumulation in hypodermal cells, and pith, (B) high magnification of (A) showing proximal ends of trichomes originating from epidermal cells (arrow head) and a glandular trichome (inset), (C) anthocyanin in epidermal and hypodermal cells, (D) free-hand transverse sections of grapevine leaf petiole without any dye infusion showing pith, vascular tissues consisting of a ring of separate vascular bundles of unequal size embedded in the parenchyma tissue resembling a stem-type organization, and cortex, (E) high magnification of (D) showing anthocyanin distribution in epidermal cells, hypodermal cells and cortex, and (F) a region of (D) with no anthocyanin accumulation in epidermal and hypodermal cells. Scale bars: 100 μm (A, D), 50 μm (B, C, E), and 40 μm (F). C- Cortex, EP- Epidermal cells, GT- Glandular trichome, HP- Hypodermal cells, C- Cortex, CT- Covering trichome, and V- Vascular bundle.

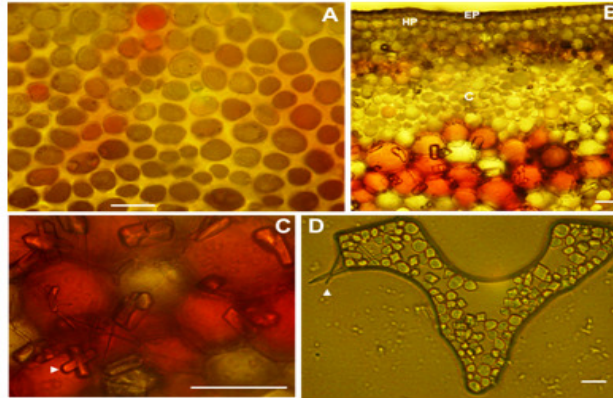


Fig 9. Free-hand transverse sections of grapevine leaf petiole without any dye infusion viewed with bright field microscopy showing cortical cells of different sizes with abundant intercellular spaces and some with anthocyanin, (B) anthocyanin accumulation in the inner cortical cells, very light accumulation in the outer cortical cells but no anthocyanin accumulation either in the epidermal or hypodermal cells, (C) high magnification of (B) showing anthocyanin in the inner cortical cells, which were overlaid with loosely distributed crystals (arrow head), (D) druse crystals trapped in an air bubble whereas some raphide crystals (arrow head) laid on the left hand side of the bubble. Scale bars: 25 μ m (A), 50 μ m (B), 50 μ m (C), and 100 μ m (D). C- Cortex.

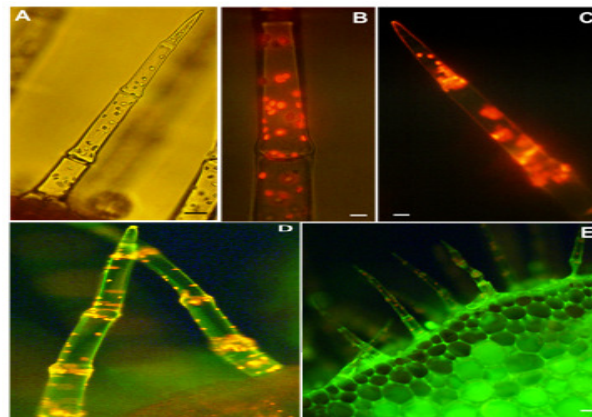


Fig 10. Achromatic covering trichomes (A) as appeared when viewed with bright field microscopy in free-hand transverse sections of African violet petiole in the absence of dye infusion, autofluorescent images (red) viewed with epifluorescence microscopy emanating from (B) proximal and (C) distal ends of trichomes; fluorescently illuminating (D) trichomes (green carboxyfluorescein-induced fluorescence) and (E) petiole epidermis, cortical cells, and trichomes. Green fluorescence is visible in the thin peripheral layer of cytoplasm adjacent to the cell wall. Scale bars: 20 μ m (A), 10 μ m (B), 10 μ m (C), 100 μ m (D), and 100 μ m (E).

DISCUSSION

The marvels of structural soundness in a range of plant organs as illustrated in this study were achieved by an ensemble of multifarious free-hand sectioning techniques with classical optical microscopy. The central architect of this microscopy combine was basic fuchsin, a cationic dye [61] that was exploited not only to elucidate hydraulic pathways in leaves but also to generate contrast for viewing cellular details in leaves, stems, and fruits. For instance, the dye distribution pattern in healthy leaves rendered its reticulate venation architecture clearly visible, which reminded of natural ramified structures such as the vascular system of animals or river basins. The very fact that both living and non-living natural systems share this feature is indicative of ramified structures conferring some advantage to the system. For instance, Bond (1989) [9] argued that the reticulate venation pattern is partly responsible for the evolutionary success of the angiosperms leading to their dominance in most temperate and tropical vegetation. Another interesting aspect was the redundancy of flow paths in the vein architecture. This is a physiologically beneficial feature as it minimizes the deleterious effect of insects and other sources of

damage (i.e. cavitation) on transport pathways, while at the same time provides a physical barrier limiting the spread of such damage [47]. Although, these natural networks have long been an object of scientific inquiry, not much is known about the physical principles that constrain vascular architecture in leaves [6, 20]. Consequently, the investigation of the formation and function of leaf venation continues to be of current interest in plant biology. The knowledge that living and non-living systems share ramified structures offers the possibility of an interdisciplinary approach to further our understanding of the leaf venation system [45], and perhaps the dye infusion technique described in this study may be complementary to this concerted effort.

Although staining of cell walls revealed cellular details in the petiole, the green filter in the microscope light path further enhanced contrast by absorbing the stained specimen color rendering the xylary fiber walls a darker grey, the secondary cell walls of the fiber cap a lighter grey, and luminescent green to middle lamellae of fiber cap cells and vessel lumens. The cell walls of the phloem fiber cap were particularly distinguishable visually. These fibers are very long and narrow cells with thick lignified cell walls [1] commonly found in monocotyledons and dicotyledons [27]. Hence, contrast

can be adjusted by selectively choosing filters that absorb varying amounts of the stain color. Because the fiber caps are located inside the innermost cortical layer and on the periphery of the central cylinder, they were first termed pericyclic fibers; however, ontogenetic studies showed that they develop from the procambrium and they were, therefore, renamed primary phloem fibers [7, 26].

Even though basic fuchsin ascends in the xylem stream, the pith cell walls were also stained presumably due to redistribution of dye from vascular tissues to pith analogous to lateral conduction of water by ray parenchyma cells towards the pith. A similar phenomenon was observed in embedded sections of trees [48]. The staining of pith walls turned out to be advantageous in further enhancing the image quality due to the fluorescent properties of basic fuchsin [28], which provided a more distinguishable and well defined structure of cell walls. In other words, the fluorescent properties of basic fuchsin generated a more steady microscopic background for a sharper delineation of cell wall structures since no projection from lower levels interfered. To my knowledge, there exists no previous reports on this phenomenon in plant tissues but a similar context can be found in animal cells wherein stained bones imparted a better quantification of microdamage under UV light rather than white light [28]. This indicated that fluorescent images of basic fuchsin-stained cells provide better structural information than bright field images.

The limited dye movement into the water-stressed leaf midrib could be due to two reasons: firstly, a lack of driving force failed to pull the dye into the leaf ensuing from desiccation of lamina, and secondly water stress-induced cavitation [19, 23, 34, 42] of an increased number of xylem vessels contributed to uneven distribution of dye in the midrib. Although cavitation was invisible in fresh sections, the limited staining of few vessels strongly supported its occurrence. So, what are some of its implications for microscopy and plant research? In the context of image quality, the uneven distribution of dye in the xylem tissues imparts a nice contrast for visualizing cellular details. From a research perspective focusing on stress physiology, one could promptly test for water stress-induced cavitation or cell collapse under negative pressure [17] providing the examiner with range of options to confirm cavitation by performing complex cryoSEM analysis or choosing between acoustic [41] and hydraulic conductance methods [53]

Unequivocally, the internal organization of cells in grapevine woody stem had a better resolution and contrast in the presence of dye, which profoundly exaggerated the dissimilarities among the distinctly organized cells of secondary conducting tissues. In other words, free-hand sections examined by this mode can provide insights into secondary growth. There are important scientific motivations to study secondary growth as it presents striking examples of plastic developmental processes such as meristem activity, tissue patterning, and cell differentiation, which are strongly influenced by environmental cues [25]. Apart from generating images of this evolutionarily ancient phenomenon of secondary growth, the simplicity of tissue observation in this manner allows for rapid and accurate statistical analysis of structural parameters of xylem and some phloem tissues. These are essential for the calculation of xylem conductivity enhancing the understanding of hydrodynamics and the grand hydraulic design of woody stems.

Except the fiber cap and secondary phloem parenchymatous cells, all secondary conducting tissues including the xylary fibers and secondary phloem fibers stained red indicating redistribution of dye from vascular tissues to these tissues. In addition to having

undergone secondary growth, the stem developed phellogen or cork cambium, which basically disconnects primary phloem including the fiber cap from internal tissues [56] accounting for the lack of radial movement of dye from the xylem into the fiber cap. Nevertheless, despite lacking stained walls, nothing was more obvious than the fiber cap, which exhibited well defined cellular boundaries resulting from the yellowish shine of the middle lamella and the light yellow color of the secondary cell wall. Collectively, they generated a color image that had natural and high contrast enabling different cell layers to be distinguished visually. For instance, the middle lamella that ensures the adhesion of a cell to its neighbors and comprising of pectic substances and, lignin, which exhibits a high intensity of yellow shine [29] was clearly visible in the fiber cap. Accordingly, higher lignin content was visualized in the middle lamellae and cell corners than in the secondary cell wall enabling direct visualization of the spatial variation of the lignin content without any chemical treatment or staining of the cell wall. Conversely, if lignin-specific stain such as safranin [54] is used, it is better to view the sections with UV light. This is because it not only shows the presence of lignin but also yields a more distinguishable and well defined structure of cell walls as evident from the pedicel of grapevine owing to the fluorescence radiating from lignified cell walls. Attached to the middle lamella is the primary cell wall on the inside of which, after reaching the definitive size, the highly structured secondary cell wall is evenly deposited in three layers, viz; S1, S2 and S3, which can be observed with transmission electron microscopy [43]. Although, secondary walls were rather observed easily, the underlying mechanisms controlling their patterned deposition are largely unknown [69]. Hence, elucidation of the mechanisms that plants evolved to produce secondary walls is undoubtedly an important issue in plant biology [68] and simple microscopy techniques such as described here could be valuable to understanding both the evolution of vascular plants and the development of different cell types.

The anatomical details discussed thus far resulted from dye infusion into the leaf or stem tissues. What if, the xylem vessels are blocked, say for instance due to tylosis wherein adjacent parenchyma cells intrude through pit-pairs and occlude the vessel lumen [38]. Tylosis is a defensive process for sealing vessel members following ethylene production [57] triggered by mechanical injury or fungal, bacterial or viral infections [55, 58, 64]. In this scenario, post-staining of free-hand sectioning with dyes such as safranin is the best way to observe internal structures as shown in this study with tylosed grapevine stems. Not only the safranin stained the lignified cell walls but it also adhered to the walls of tylosed parenchymatous tissues. This was not surprising as safranin stains a variety of cell components including primary wall [31]. Observing cells in post-stained sections with safranin using transmitted light has long been the tradition [40]. However, knowing that safranin fluorescently labels the cell walls [3], it was possible to obtain sharper images with additional structural information. For instance, in the pedicels, the yellow fluorescence emanating from the vascular tissues indicated the presence of lignin in the secondary cell walls since regions of low levels of lignin stained with safranin fluoresce yellow [3]. On the other hand, regions with high levels of lignin as found in pear sclereids fluoresced red or green [3], whereas in the middle lamellae of pine tracheids, it fluoresced red or orange [8]. The fluorescent images of pedicels strongly supported the notion that fluorescing safranin-stained cells reveal differences in chemical composition. Thus, this microscopy technique not only generates fine cellular details but also

serves as an efficient method for screening variations in cell wall composition that may arise from a whole raft of factors such as mutation, genetic modification, biotic and abiotic stresses etc. without counterstaining as required for bright field microscopy. Similarly, the fluorescent properties of safranin are used by forensic scientists in processing latent human finger prints [62].

Owing to the soft mesocarp and high sugar accumulation in grape berries, the conventional immersion protocols using fixatives do not work well for observing their internal structures [24]. Such a challenge can be resolved to a great extent by infusing the dye especially into young berries. The red staining of the vascular walls embedded in the translucent mesocarp imparts a nice contrast. On the other hand, the ripened berries cannot be passively infused with dye as there exists no driving force (negative hydrostatic gradient) for the dye to pull into the berry [13, 35]. This does not mean that the internal structures of ripened berries cannot be visualized. In such scenarios the pigmented venation pattern rendered by anthocyanin accumulation in the epidermal cells overlying the veins as commonly observed in *Antirrhinum majus* flowers [50] could be used to introduce contrast in cross sections. Analogous to this flower, grape berries exhibit strong vasculature patterning (pigment associated with the septum and brush cells surrounding the veins; brush – opaque tissues that remains attached to the pedicel after it has been removed from the fruit), which provided the necessary contrast to observe the fundamental internal structures. For instance, the translucency of the flesh (mesocarp) due to flooding of air spaces or the free spaces with apoplastic sap [65] was clearly visible against the pigmented septum and brush. Furthermore, the translucency of the mesocarp in combination with brown coloration of seeds revealed the seed morphological details to a great extent. Pigmentation due to anthocyanin accumulation also occurs in petioles of leaves [30] as shown in this study with grapevine and African violet petioles, which conveyed fine details of internal tissues. One striking feature of grapevine is that they accumulate increased amount of crystals as druses and raphides in almost all of their organs [22], hence this species can serve as a good model for examining the process of biomineralisation and the morphology and ultrastructure of crystals. For instance, the individual facets of druse crystals displaying several distinct shapes suggested that druse microstructure may be species specific and potentially could be used as a taxonomic character; however, this particular realm of crystal formation is yet to be pursued in depth.

CFDA, a non-fluorescent dye has been used extensively in plant research as a marker for symplasmic transport [32] and to test the viability of cells [11]. It enhanced contrast in free-hand sections by crossing cell membranes passively in acetate form and then it was cleaved by cytosolic enzymes [36]. The resultant free building up of fluorescent and impermeant carboxyfluorescein in the cytoplasm caused it to fluoresce green throughout [67] generating brilliantly visible internal details in the fluorescent images. These trichomes derived from the epidermal layer are either single or grouped multicellular, uniseriate structures, which occur at the same level as the epidermal surface or on a multicellular emergence [5, 12] are of great importance to plant survival and adaptation [66]. Most importantly, they serve as a model system in cell differentiation studies [49]. Hence, it is not surprising to see them as the subject of routine investigation in taxonomical, anatomical and physiological studies. One intriguing aspect of the image obtained in this study was pyrenodeous (wart-like) surface markings on the cell wall that emitted reddish autofluorescence, but switched to yellowish

fluorescence after staining with CFDA. A similar phenomenon was observed in leaf trichomes of *Cistus salvifolius* L. that exhibited orange-red autofluorescence but emitted yellow fluorescence when stained with the Naturstoff reagent attributed to accumulation of flavonoids in the trichomes [60]. Whether or not the African violet trichomes accumulated flavonoids or other fluorescent compounds could not be ascertained including the chemical and morphological characteristics of warty structures as these measures were beyond the scope of this study. Nevertheless, in light of the role played by the warty structures in enhancing the contrast of the image, these structures are worth our attention. Unfortunately, not much is known about them other than their description in few studies [(e.g. 2]. Nevertheless, one study hypothesized that these structures are due to local depositions of cellulose, cutin etc. [21], which have been known to autofluoresce [33]. Other potential biochemical sources of autofluorescence in trichomes include secondary metabolites and compounds such as proteins, mineral elements, and glutathiones [16, 51].

CONCLUSIONS

Although free-hand sectioning is rather a simple procedure, continuous efforts are being made to simplify it further for faster results. In that context, this study represents a remarkable example of imparting relatively a new dimension to this technique that holds the greatest promise for significantly contributing to a rapid and safe examination of cellular structures in plant tissues. This ensemble of simple techniques presented in this study certainly constitutes another tool in the tool box for rapid high quality snapshot of cells in their native physiological context. The main advantage of this method is that a range of tissues from different plant organs can be examined readily to gain a quick critical insight into the fundamental nature of cellular and tissue function. Particularly, many researchers who have no previous microscopy experience may now use this technique to complement their research. As progress continues and challenges are overcome, this technique will continue to evolve and serve as an invaluable approach for a safer and faster learning of cellular structures.

REFERENCES

- [1] R. Aloni. 1976. "Polarity of induction and pattern of primary phloem fiber differentiation in coleus," *American Journal of Botany*, vol. 63, pp. 877-889.
- [2] M, Ancev, V, Goranova V, 2006. "Trichome morphology of eleven genera of the tribe *Alysseae* (*Brassicaceae*) occurring in Bulgaria," *Willdenowia*, 36, pp. 193-204.
- [3] G, Angeles, S. A. Owens, F. W. Ewers. 2004. "Fluorescence shell: a novel view of sclereid morphology with the confocal laser scanning microscope," *Microscopy Research and Technique*, vol. 63, pp. 282-288.
- [4] M. Archetti, T. F. Doring, S. B. Hagen, N. M. Hughes, S. R. Leather, D. W. Lee, S. Lev-Yadun, Y. Manetas, H. J. Ougham, P. G. Schaberg, G. Thomas, 2008. "Unravelling the evolution of autumn colours: an interdisciplinary approach," *Trends in Ecology and Evolution*, vol. 24, pp. 166-173.
- [5] W. Barthlott, S. Wiersch, Z. Colic, K. Koch. 2009. "Classification of trichome types within species of water fern *Salvinia*, and the ontogeny of egg-beater trichomes," *Botany* vol. 87, pp. 830-

836.

- [6] A. Bejan. 1997. "Constructal tree network for fluid flow between a finite size volume and one source or sink,". *Revue Generale de Thermique*, vol. 36, pp. 592-604.
- [7] A. Blyth A.1958. "Origin of primary extraxylary stem fibers in Dicotyledons." *University of California Berkeley Publication* vol. 30, pp. 145-232.
- [8] W. J. Bond. 1989. "The tortoise and the hare: ecology of angiosperm dominance and gymnosperm persistence," *Biological Journal of the Linnean Society*, vol. 36, pp. 227-249.
- [9] J. Bond, L. Donaldson, S. Hill, K. Hitchcock K. 2008. "Safranin fluorescent staining of wood cell walls," *Biotechnic and Histochemistry*, vol. 83, pp. 161-171.
- [10] B. R. Bondada, D. M. Oosterhuis, S. D. Wullschleger, K. S. Kim, W. H. Harris. 1994. "Anatomical considerations related to photosynthesis in cotton leaves, bracts, and the capsule wall," *Journal of Experimental Botany* vol. 45, pp. 111-118.
- [11] B. R. Bondada, M. Keller, G. Hall. 2009. "Compositional and anatomical characterization of SOUR berry." Proceedings of the International GIESCO Symposium, July 12-16, Davis, CA.
- [12] B. R. Bondada, D. M. Oosterhuis. 2000. "Comparative epidermal ultrastructure of cotton (*Gossypium hirsutum* L.) leaf, bract, and capsule wall." *Annals of Botany*, vol. 86, pp. 1143-1152.
- [13] B. R. Bondada, M. A. Matthews, K. A. Shackel KA. 2005. "Functional xylem in grapevine berries." *Journal of Experimental Botany*, vol. 56, pp. 2949-2956.
- [14] B. R. Bondada. 2010a "Micromorpho-anatomical examination of 2, 4-D phytotoxicity in grapevine leaves." *Journal of Plant Growth Regulation* DOI 10.1007/s00344-0109183-7.
- [15] B. R. Bondada. 2010b. "Analysis of anomalous structures, growth characteristics, and nutritional composition of 2, 4-D drift phytotoxicity to grapevine (*Vitis vinifera* L.) leaves and clusters." *Journal of the American Society for Horticultural Science*.
- [16] F. Bourgis, S. Roje, M. L. Nuccio, D. B. Fisher, M. C. Tarczynski, C. Li, C. Herschbach, H. Rennenberg, M. J. Pimenta, T. Shen, D. A. Gage, A. D. Hanson. 1999. "S-methylmethionine plays a major role in phloem sulfur transport and is synthesized by a novel type of methyltransferase." *Plant Cell*, vol. vol. 11, pp. 1485-1498.
- [17] T. J. Brodribb, N. M. Holbrook. 2007. "Forced depression of leaf hydraulic conductance in situ: effects on the leaf gas exchange of forest trees." *Functional Ecology*, vol. 21, pp. 705-712.
- [18] M. C. Brundrett, G. Murase, B. Kendrick. 1990. "Comparative anatomy of roots and mycorrhizae of common Ontario trees." *Canadian Journal of Botany*, 68, vol. pp. 551-578.
- [19] B. Choat, M. C. Ball, J. G. Luly, J. A. M. Holtum. 2005. "Hydraulic architecture of deciduous and evergreen dry rainforest tree species from north-eastern Australia." *Trees—Structure and Function*, vol. 19: pp. 305–311.
- [20] F. Corson, A. Adda-Bedia, A. Boudaoud. 2009. "In silico leaf venation networks: Growth and reorganization driven by mechanical forces." *Journal of Theoretical Biology*, vol. 259, pp. 440-448.
- [21] P. Dayanandan, P. B. Kaufman PB. 1976. "Trichomes of *Cannabis sativa* L. (Cannabaceae)." *American Journal of Botany*, vol. 63, pp. 578-591.
- [22] S. DeBolt, J. Hardie, S. Tyerman, C. M. Ford. 2004. "Composition and synthesis of raphide crystals and druse crystals in berries of *Vitis vinifera* L. cv. Cabernet Sauvignon: Ascorbic acid as precursor for both oxalic and tartaric acids as revealed by radiolabelling studies." *Australian Journal of Grape and Wine Research*, vol. 10, pp. 134-142.
- [23] S. Delzon, C. Douthe, A. Sala, H. Cochard. 2010. "Mechanism of water-stress induced cavitation in conifers: bordered pit structure and function support the hypothesis of seal capillary-seeding." *Plant Cell and Environment*, vol. 33, pp. 2101-2111.
- [24] P. Diakou, J. P. Carde. 2001. "In situ fixation of grape berries." *Protoplasma*, vol. 218: pp. 225-235.
- [25] J. Du, A. Groover. 2010. Transcriptional Regulation of Secondary Growth and Wood Formation. *Journal of Integrative Plant Biology*, vol. 52, pp. 17-27.
- [26] K. Esau. 1943. "Vascular differentiation in the vegetative shoot of *Linum*. III. The origin of the bast fibers." *American Journal of Botany*, vol. 30, pp. 579-586..
- [27] K. Esau. 1969. The phloem. In *Encyclopedia of plant anatomy*. In: Zimmermann W, Ozenda P, Wulff HD, eds. Berlin:Borntraeger, pp. 2-10.
- [28] T. Frisch, M. S. Sørensen, P. Bretlau. 2001. "Recognition of basic fuchsin prestained microfissures of intravital origin with fluorescence microscopy: validation of a shortcut." *European Archives of Otorhinolaryngology*, vol. 258, pp. 55-60.
- [29] N. Gierlinger, M. Schwanninger. 2006. "Chemical Imaging of Poplar Wood Cell Walls by Confocal Raman Microscopy." *Plant Physiology*, vol. 140, pp. 1246-1254.
- [30] B. J. Glover, H. M. Whitney. 2010. "Structural colour and iridescence in plants: the poorly studied relations of pigment colour." *Annals of Botany*, vol. 105, pp. 505–511.
- [31] J. D. Gray, P. Kolesik, P. B. Hoj, B. G. Coombe. 1999. "Confocal measurement of the three-dimensional size and shape of plant parenchyma cells in a developing fruit tissue." *Plant Journal*, vol. 19, pp. 229-236.
- [32] N. Grignon, B. Touraine, M. Durand. 1989. "6 (5) Carboxyfluorescein as a tracer of phloem sap translocation." *American Journal of Botany*, vol. 76: pp. 871-877.
- [33] S. S. Huang, B. K. Kirchoff, J. P. Liao. 2008. "The capitate and peltate glandular trichomes of *Lavandula pinnata* L. (Lamiaceae): histochemistry, ultrastructure, and secretion." *Journal of the Torrey Botanical Society*, vol. 135, pp. 155-167.
- [34] D. M. Johnson, F. C. Meinzer, D. R. Woodruff, K. A. McCulloh. 2009. "Leaf xylem embolism, detected acoustically and by cryo-SEM, corresponds to decreases in leaf hydraulic conductance in four evergreen species." *Plant, Cell and Environment*, vol. 32, pp. 828–836.
- [35] M. Keller, J. P. Smith, B. R. Bondada. 2006. "Ripening grape berries remain hydraulically connected to the shoot." *Journal of Experimental Botany*, vol. 57, pp. 2577-2587.

- [36] M. Knoblauch, A. J. E. van Bel. 1998. "Sieve tubes in action." *Plant Cell*, 10, vol. pp. 35-50.
- [37] S. Krishnan, P. Dayanandan. 2003. "Structural and histochemical studies on grain-filling in the caryopsis of rice (*Oryza sativa* L.)." *Journal of Bioscience*, vol. 28, pp. 455-469.
- [38] S. Lev-Yadun S. 2001. "Intrusive growth – the plant analog of dendrite and axon growth in animals." *New Phytologist*, vol.150, pp. 508–512.
- [39] A. Lux, S. Morita, J. Abe, K. Ito. 2005. "An improved method for clearing and staining free-hand sections and whole-mount samples." *Annals of Botany*, vol. 96, pp.989-996.
- [40] Y. Ma, V. K. Sawhney, T. A. Steeves. 1993. "Staining of paraffin-embedded plant material in safranin and fast green without prior removal of the paraffin." *Canadian Journal of Botany*, vol. 71, pp. 996-999.
- [41] J. A. Milburn. 1973. "Cavitation in *Ricinus* by acoustic detection: Induction in excised leaves by various factors." *Planta*, vol. 110, pp. 253-265.
- [42] A. Nardini, M. T. Tyree, S. Salleo. 2001. "Xylem cavitation in the leaf of *Prunus laurocerasus* and its impact on leaf hydraulics." *Plant Physiology*, vol. 125, pp.1700–1709.
- [43] C. Plomion, G. G. Leprovost, A. Stokes. 2001. "Wood formation in trees." *Plant Physiology*, vol. 127, pp. 1513-1523.
- [44] C. L. Rieder, A. Khodjakov. 2003. "Mitosis through the microscope: Advances in seeing inside live dividing cells." *Science*, vol. 300, pp. 91-96.
- [45] A. Roth-Nebelsick, D. Uhl, V. Mosbrugger, H. Kerp. 2001. "Evolution and function of leaf venation architecture: A review." *Annals of Botany*, vol. 87, pp. 553-566.
- [46] S. E. Ruzin. 1999. *Plant Microtechnique and Microscopy*, Oxford: Oxford University Press.
- [47] S. Salleo, A. Nardini, L. M. Gullo. 1997. "Is sclerophylly of mediterranean evergreens an adaptation to drought?" *New Phytologist*, vol. 135, pp. 603–312.
- [48] Y. Sano, Y. Okamura, Y. Utsumi. 2005. "Visualizing water-conducting pathways of living trees: selection of dyes and tissue preparation methods." *Tree Physiology*, vol. 25, pp. 269-275.
- [49] S. Schellman, M. Hulskamp. 2005. "Epidermal differentiation: Trichomes in *Arabidopsis* as a model system." *International Journal of Developmental Biology*, vol. 49, pp. 579-584.
- [50] Y. Shang, J. Venail, S. Mackay, P. C. Bailey, K. E. Schwinn, P. E. Jameson, C. R. Martin, K. M. Davies. 2010. "The molecular basis for venation patterning of pigmentation and its effect on pollinator attraction in flowers of *Antirrhinum*." *New Phytologist*, 10.1111/j.1469-8137.2010.03498.
- [51] T. Sinlapadech, J. Stout, M. O. Ruegger, M. Deak, C. Chapple. 2007. "The hyper-fluorescent trichome phenotype of the *brt1* mutant of *Arabidopsis* is the result of a defect in a sinapic acid: UDPG glucosyltransferase." *Plant Journal*, 49, pp. 655-658.
- [52] M. T. Smith. 1990. "Chloral hydrate warning." *Science*, 250, p. 359.
- [53] J. S. Sperry, J. R. Donnelly, M. T. Tyree. 1988. "A method for measuring hydraulic conductivity and embolism in xylem." *Plant, Cell and Environment* vol. 11, pp. 35-40.
- [54] E. Srebotnik, K. Messnera. 1994. "A simple method that uses differential staining and light microscopy to assess the selectivity of wood delignification by white rot fungi." *Applied and Environmental Microbiology*, vol. 60, pp. 1383-1386.
- [55] J. F. Stevenson, M. A. Matthews, L. C. Greve, J. M. Labavitch, T. L. Rost. 2004. "Grapevine Susceptibility to Pierce's Disease II: Progression of Anatomical Symptoms." *American Journal of Enology and Viticulture*, vol. 55, pp. 238-245.
- [56] J. F. Stevenson, M. A. Matthews, T. L. Rost. 2005. "The developmental anatomy of Pierce's disease symptoms in grapevines: Green islands and matchsticks." *Plant Disease*, vol. 89, pp. 543-548.
- [57] Q. Sun, T. L. Rost, M. S. Reid, M. A. Matthews. 2007. "Ethylene and not embolism is required for wound-induced tylose development in stems of grapevines." *Plant Physiology*, vol. 145, pp. 1629-1636.
- [58] Q. Sun, T. L. Rost, M. A. Matthews. 2008. "Wound-induced vascular occlusions in *Vitis vinifera* (Vitaceae): Tyloses in summer and gels in winter." *American Journal of Botany*, vol. 95, pp.1498-1505.
- [59] P. W. Talbot. 1955. "Detection of vascular tissues available for water transport in the hop by colorless derivatives of basic dyes." *Nature*, vol. 175, p. 510.
- [60] M. Tattini, P. Matteini, E. Saracini, M. L. Traversi, C. Giordano, G. Agati. 2007. "Morphology and biochemistry of non-Glandular trichomes in *Cistus salvifolius* L. leaves growing in extreme habitats of the Mediterranean basin." *Plant Biology*, vol. 9, pp. 411-419.
- [61] T. Umebayashi, Y. Utsumi, S. Koga, S. Inoue, Y. Shiba, K. Arakawa, J. Matsumara, K. Oda. 2007. "Optimal conditions for visualizing water-conducting pathways in a living tree by the dye injection method." *Tree Physiology*, vol. 27, pp. 993-999.
- [62] United States Department of Justice. 1994. "Chemical formulas and processing guide the developing latent finger prints." Washington, DC: United States Department of Justice."
- [63] P. J. R. Uwins, M. Murray, R. J. Gould, 1993. "Effects of four different processing techniques on the microstructure of potatoes: comparison with fresh samples in the ESEM." *Microscopy Research and Technique*, vol. 25, pp. 412-418.
- [64] G. E. VanderMolen, C. H. Beckman, E. Rodehorst. 1987. "The ultrastructure of tylose formation in resistant banana following inoculation with *Fusarium oxysporum* f. sp. *Cubense*." *Physiological and Molecular Plant Pathology*, vol. 31, pp. 185–200.
- [65] H. Wada, K. A. Shackel, M. A. Matthews. 2008. "Fruit ripening in *Vitis vinifera*: apoplastic solute accumulation accounts for pre-veraison turgor loss in berries." *Planta*, vol. 227, pp. 1351-1361.
- [66] G. J. Wagner, E. Wang, R. W. Shepherd. 2004. "New approaches for studying and exploiting old protuberance, the plant

trichome." *Annals of Botany*, vol. 93, pp. 3-11.

- [67] K. M. Wright, K. J. Oparka. 1996. "The fluorescent probe HPTS as a phloem-mobile, symplastic tracer: an evaluation using confocal laser scanning microscopy." *Journal of Experimental Botany*, vol. 47, pp. 439-445.
- [68] R. Zhong, C. Lee, J. Zhou, R. L. McCarthy, Z. H. Ye. 2008. "Battery of transcription factors involved in the regulation of secondary cell wall biosynthesis in Arabidopsis." *Plant Cell*, vol. 20, pp. 2763-2782.
- [69] R. Zhong, Z. H. Ye. 2009. "Secondary Cell Walls. In: *Encyclopedia of Life Sciences (ELS)*. Chichester: John Wiley & Sons, Ltd., 1-9.